Synthesis, Structural and Microstructural Analysis of Sol-gel prepared Lithium – Doped ZnO Ceramics ($Zn_{1-x}Li_xO$)

ALI, S. O.[1] **& UMAR, A**[1]
[1]Physics Department,
Federal University of Technology, Minna, Niger State, Nigeria
E-mail: eldonogozimaco@gmail.com **Phone No:** +234-906-0438898

Abstract

Structural and microstructural properties of $Zn_{1-x}Li_xO$ *(*$0.00 \leq x \leq 0.5$ *) ceramics synthesised by sol-gel technique were investigated. The samples were synthesised by stirring the solutions of LiCl and Zinc acetate dihydrate in a magnetic stirrer for 6 hours. The resulting solution was aged for 24 hours, evaporated at 90* ^{0}*C, calcined and sintered at 800* ^{o}*C for 8 hour and 1200* ^{o}*C for 10 hours. Structural analysis from XRD reveals that the prepared samples are polycrystalline in nature having hexagonal wurtzite structure. It was observed that the 2θ position shifted to lower and higher angles. The average crystallite size was estimated using Scherrer's equation, Williamson-Hall model and Size-Strain plot. The average crystallite size in all the models, decreased with increase in Lithium concentration. The lattice parameters a and c decreased with lithium doping. The a/c (ratio) was fairly constant indicating that the prepared material maintained their hexagonal structure in spite of Lithium doping. Morphology evolution was observed in the SEM images; from non-uniform distributed spherical shaped grains with much porosity and agglomeration at x=0, to rod-like agglomerated grains with less porosity at x=0.3.There was a decrease in grain size with increase in Lithium doping, with respect to grain size, the optimum doping concentration was 0.5 mol. This gave the lowest grain size with high potential for piezoelectric application.*

Introduction

ZnO is a multifunctional material (Lou, 1991; Segets*et al.*, 2009) with unique physical and chemical properties, such as high chemical stability, high electrochemical coupling coefficient, broad range of radiation absorption and high photo stability). It is a group II-VI compound; this is because zinc is in group II while oxygen is in group VI in the periodic table. The bond in ZnO is largely ionic which explains its strong piezoelectric properties. The unique and fascinating properties of II-VI compound semiconductors have triggered tremendous motivation among scientists to explore the possibilities of using them in industrial applications (Sajjad, 2008) such as in transducer, electrical and medical science. Zinc Oxide crystallizes in three forms: cubic zinc –blende and cubic Rocksalt.

Zinc Oxide is a piezoelectric material with the highest piezoelectricity among the tetrahedral crystals due to its high electromechanical coupling (Dai *et al.*, 2013). It also has the highest piezoelectric tensor among the tetrahedral semiconductor (Corsol *et al.*, 1994). This property makes it a technologically important material to be applied in devices that require large electromechanical coupling.

Lead compounds have been considered as one of the most hazards and cumulative environmental pollutant capable of affecting all biological systems adversely. Exposure to Lead could produce various deleterious effects on hematopoietic, renal, reproductive and central nervous system (Patra *et al.*, 2011; Kalia & Flora, 2005). A high level of lead could result in animal reproductive failure (Ahmad *et al.*, 2008), Encephalopathy (a progressive degeneration of certain parts of the brain), convulsion and Coma (Flora *et al* 2006; Pearce, 2007) and other health and environmental problems. Consequently, there has been a strong drive over the years to replace Lead in electronics and other household materials. Suffice to say that the major sources of Lead exposure are Lead batteries, Lead piezoceramics, Lead gasoline and Lead paints.

Lithium-doped Zinc Oxide is an excellent piezoelectric material that has several applications. Firstly it can be used to replace highly toxic Lead (Pb) materials in electronics in order to reduce environmental pollution. Secondly, Lithium -doped Zinc oxide can be applied in transducers for converting untapped environmental mechanical energy into electrical energy that is used in ultrasound equipment, thereby providing solution to myriads of our energy need. It can also be used in voice recognition technology that converts sound energy into electrical signal in computers. Due to Zinc oxide biocompatibility, Lithium-doped Zinc oxide could find wide Therapeutic and diagnostic applications in ultrasonic imaging were its non-toxic nature could guarantee the safety of the patient and the examiner, in surgical cutting, foetal heartbeats monitor and in cancer treatment .Other fields where lithium -doped Zinc oxide Piezoelectric material could be used are in micro actuators, MEMs (micro electromechanical systems), energy harvesters and nanogeerators. In communication and Aerospace Technology, lithium doped Zinc Oxide Piezoelectric Material could be used in satellite communication system because of its excellent stability and high sensitivity (Prasad *et al*, 2005).

The last two decades has witnessed a great resurgence of interest in Zinc Oxide due to its numerous properties such as optical, electrical, magnetic and piezoelectricity. These vast properties have remained underutilized as a result of problems associated with synthesis. Some of the Challenges associated with synthesizing doped and undoped ZnO include careful selection of the dopant concentration, presence of impurities in the synthesized materials leading to the formation of secondary phase, control of PH and temperature during synthesis. Several Methods such as hydrothermal, mechanochemical, precipitation, microwave and sol-gel have been used to prepare doped and undoped Zinc Oxide. Sol-gel synthesis method have a great potential of fully harnessing the underutilized properties of Zinc Oxide due to its ability to control and modify the surface of Zinc Oxide through doping and the possibility of producing doped and undoped Zinc Oxide with high level of purity and single phase.

Lastly, Lithium-doped piezoelectric material are used in household goods such as in cigarette lighter, Piezo buzzer in burglar alarms systems, ultrasonic humidifiers, electric toothbrush and musical instrument. In this study, structural characterization of phase composition and crystallite size using XRD based Scherrer Equation and Williamson- Hall analysis was used. Morphology of the samples was determined by grain size and SEM, elemental composition based on XRF.

Methodology

Composition of the precursors

Sol-gel method was used in synthesising the starting material in this study. The starting materials used were Zinc acetate dihydrate Zn $(CH_3COO)_2.2H_2O$, lithium chloride and butanol (used as a solvent). From equation 1.0 and 2.0, compound Zn $(CH_3COO)_2.2H_2O$ and LiCl were synthesised for the following compositions: ZnO,$Zn_{0.7}Li_{0.3}O$, $Zn_{0.6}Li_{0.4}O$ and $Zn_{0.5}Li_{0.5}O$.

Calculation of concentration of Lithium

The concentration of Lithium was calculated using equation

$$N = \frac{Li_{x(mol)}}{LiCl} K \qquad (1.0)$$

where N is the concentration of Lithium in mol, K is a multiplication factor while the concentration of Zinc was calculated using equation (2.0)

$$M = \frac{Zn_{1-x(mol)}}{Zn(CH3COO)_2.2H_2O} K \qquad (2.0)$$

where M is the concentration of Zinc in mol.

Synthesising of Li-doped ZnO

All the chemicals used in this synthesis (Zn $(CH_3COO)_2.2H_2O$, LiCl and Butanol) were of analytical grade. The various compositions of the reactants were first weighted out using analytical balance. 100 ml of butanol was measured with a measuring cylinder into beaker and stirred in a magnetic stirrer. For Li concentration of 0.3 mol. a solution of Lithium Chloride was made by dissolving a stoichiometric amount of Lithium Chloride solute in 50 ml of distilled water. The resulting solution was added gently to 100 ml of butanol being stirred in a magnetic stirrer. The solution of zinc acetate dihydrate was prepared by dissolving a stoichiometric amount of Zinc Acetate dehydrates in 50 ml of butanol. The solution formed was added slowly to the mixture being stirred at room temperature. A drop of concentrated $H_2SO_4$was added to the mixture after stirring it for 30 minutes which acts as a stabilizer. The mixture was stirred for six hours in a magnetic stirrer after which it was left to age for 24 hours before evaporation was achieved at a temperature of 90°C in an oven. Calcination which is a process used to eliminate volatile materials like water and other impurities was carried out at a temperature of 800°C for eight hours using Carbolite RHF 1600 furnace. All the above processes were carried out at Chemical Engineering Department, Federal University of Technology, Gidan Kwanu, Minna, Nigeria. The sintering of the powdered samples was achieved at a temperature of 1200°C for ten hours at the Engineering Workshop Department at Science Complex SCHESTCO, Abuja. These processes were repeated for other concentrations (0.4 mol. and 0.5mol.) of lithium. X- ray diffractometer (XRD D8, advance BRUKER AXS, 40kV, 40mA) with Cu Ka (lamda = 1.540598 A. 2 that range from 20^0 to 90^0 with scan step and acquisition time of 0.034^0 and 0.5 s/ step) characterisation of the material was done at Ithemba Labs, South Africa. Morphology and the microstructural analysis were done using High Resolution Scanning

Electron Microscopy (HRSEM, Zeiss Auriga), at the electron microscope unit, department of Physics, University of Western Cape, South Africa.

Results and Discussion

Result for X-ray diffraction (XRD)

XRD pattern of the synthesised $Zn_{1-x}Li_xO$ ($(0.00 \le x \le 0.50)$) are depicted Figure 1.0 The patterns confirmed that the prepared ceramics are polycrystalline with single phase wurtzite hexagonal structure which is in agreement with the reference pattern of Joint Committee on Powder Diffraction Standard JCPDS data (card ID- 36-1451) in Figure 2.0. The patterns are also in agreement with the reports of other workers who prepared Lithium doped zinc Oxide using similar method (Khan *et al*., 2003; Du *et al*., 2005; Rakkesh and Balakumar, 2016).

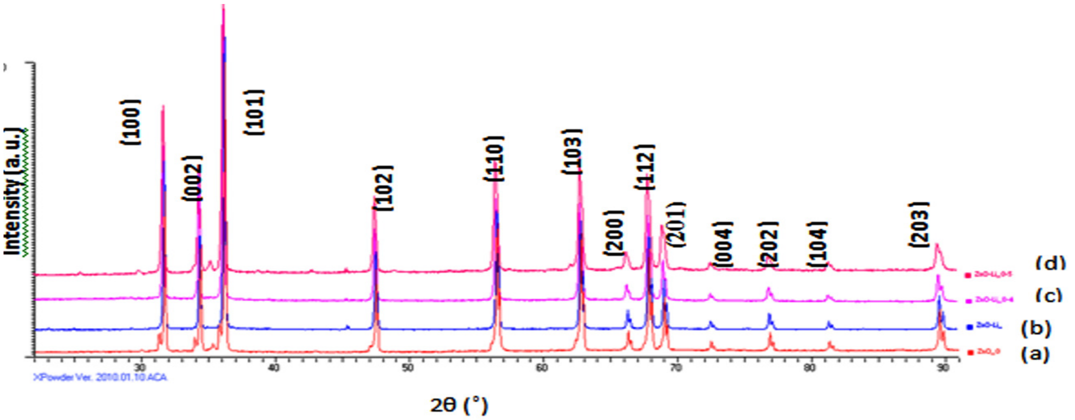

Figure 1.0: X-ray Diffraction pattern of $Zn_{1-x}Li_xO$ $(0.00 \le x \le 0.50)$) ceramics at diffraction angular range of $20^0 \le 2\theta \le 90^0$ (a) undoped Zinc Oxide(x = 0.00) (b) x = 0.3 (c) x = 0.4 (d) x = 0.5

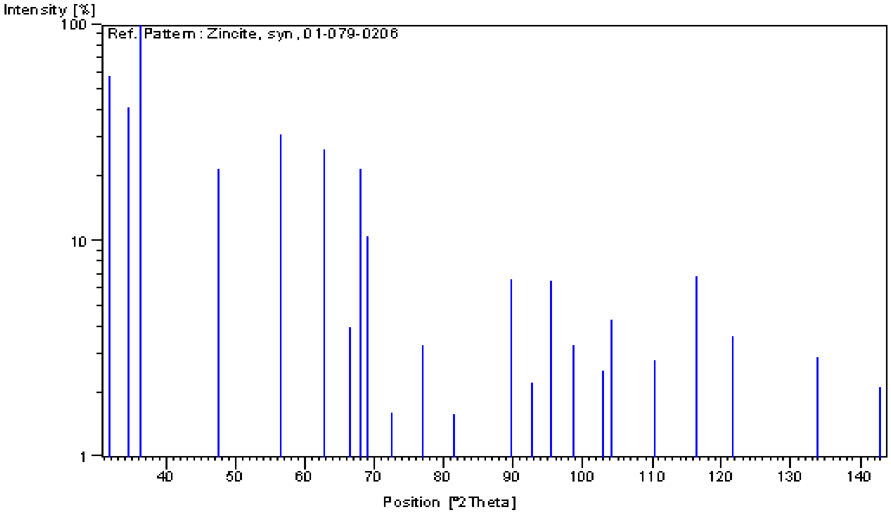

Figure 2.0: Joint committee on powder diffraction standard (JCPDS) data (card ID: 36-1451) with diffracting angle measured in the angular range of
$30^0 \le 2\theta \le 150^0$

The phases remained unchanged with the increase of dopant content from 0 to 0.5 mol as shown by Figure 4.1 (a-d).The strongest observed peaks occur at (100), (002), (101), (102), (110), (103), (112), (201) and (203) reflection planes. By doping ZnO with Lithium, the Lithium atoms occupy the Zn sites in the ZnO lattice due to their comparable ionic radii (Lina *et al*., 2010). It was observed that the intensity of (101), (102), and (110) planes increased as a result of Lithium doping at the concentration of 0.3. As the doping concentration of Lithium increases, the intensity of (100), (002) and (200) decreased consistently. This is due to the substitution of Li^+ ions of ionic radius of (0.68 Å) with Zn^{2+} ions which has ionic radius of (0.74 Å). Other researchers also reported similar result (Bilgin, 2009). It was observed that the peak positions shifted to lower angle and then to higher angles as a result of Lithium doping in agreement with earlier report (Ardyanian and Sedigh, 2013). The shifting to higher and lower angles is illustrated in Figure 3.0. The figure shows that x = 0.00 and x = 0.40 (mol) shifted to lower angles while x = 0.30 and 0.50 (mol) shifted to higher angles. The shift to higher angles is an indication of decrease lattice parameters due to replacement of smaller Li^+ ions at Zn^{2+}.The shifts observed in the 2θ positions were due to the broadening of the peaks positions as a result of Lithium doping.

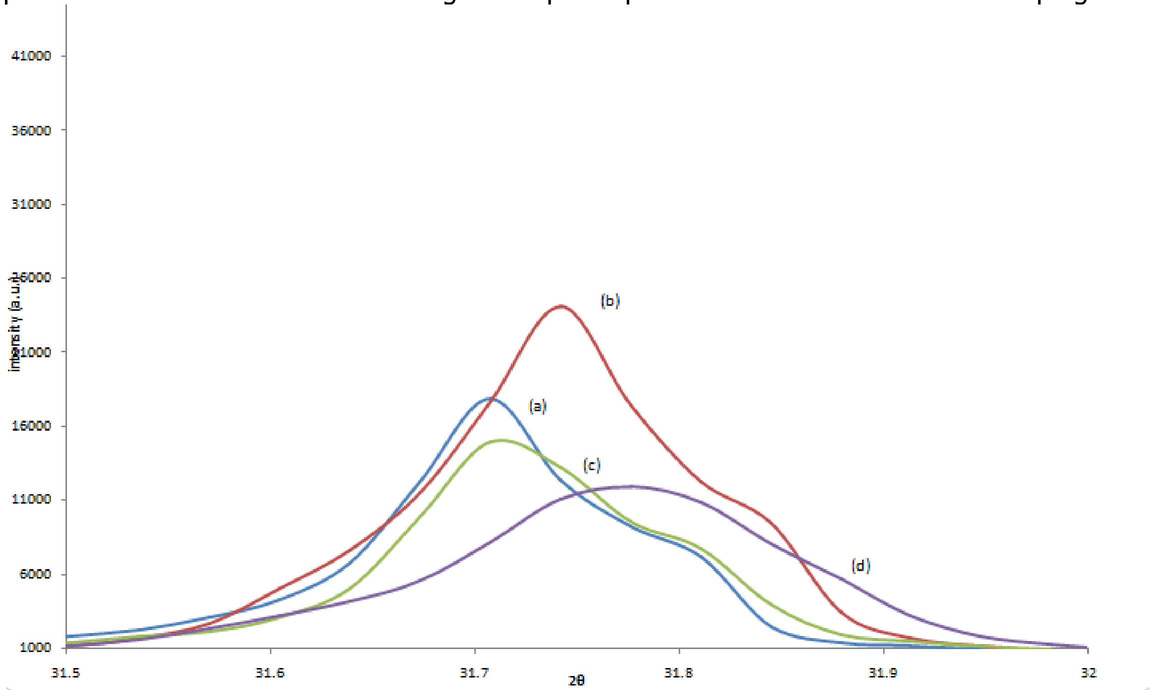

Figure 3.0: graph of intensity versus 2θ for 100 plane (a) x=0 at 31.7075° (b) x=0.3 at 31.7418° (c) x=0.4 at 31.7075° (d) x=0.5 at 31.8447°

Zeng *et al*. (2005) and Bilgin (2009) attributed this to competition between compressive stress and tensile stress in the lattice structure of Zinc Oxide as a result of substitution of Li atoms at the interstitials and Zn sites respectively. The incorporation of Lithium atoms in the interstitial and lattice site of ZnO could lead to the segregation of insoluble Li atoms at the grain boundaries thereby suppressing the growth of $Zn_{1-x}Li_xO$ (Nayak *et al*., 2009).

Estimation of the crystallite size and micro strain

The average crystallite size(s) and the microstrain were calculated utilising:

Scherrer equation

$$D = \frac{k\lambda}{\beta \cos\theta} \qquad (3.0)$$

Williamson-Hall (W-H) equation

$$\beta \cos\theta = \frac{k\lambda}{D} + c\varepsilon \sin\theta \qquad (4.0)$$

Size–strain (S-S) equation

$$B \cos\theta = \frac{k\lambda}{D} (d^2 \beta \cos\theta) + \sqrt{\frac{\varepsilon_a}{2}} \qquad (5.0)$$

The average crystallite size(s) were estimated using the most prominent peak (101) plane for Scherrer equation. The result for the Scherrer's crystallite size is presented in Figure 7.0 and it is clearly shown that the crystallite size decreases as a result of increase in FWHM with dopant concentration. This is attributed to the fact that Li^+ ions with small ionic size have replaced Zn^{2+} ions with larger ionic size.

The average crystallite size of the undoped Zinc Oxide is calculated as 66.56 nm. As the dopant concentration increased, there is a systemic decrease in the crystallite size from 66.56, 52.02, 52.13 and 40.54 nm respectively. This shows that the incorporation of Lithium atoms inhibits the growth of ZnO crystallites (Rakkesh and Balakuma, 2014).

Table 1.0 show the Full Width at Half Maximum (FWHM), 2θ position and the Scherrer's crystallite size.

Table 1.0: Peak position (2θ), FWHM (β) at (101) plane and average crystallite size (D)

Sample	2θ (degree)	$\beta x 10^3$ (radians)	D (nm)
ZnO	36.201	2.19	66.50
$Zn_{0.7}Li_{0.3}O$	36.235	2.64	55.02
$Zn_{0.6}Li_{0.4}O$	36.201	2.80	52.13
$Zn_{0.5}Li_{0.5}O$	36.270	3.60	40.54

Table 1.0 show that the FWHM increased consistently as a result of broadening of the diffraction peak and consequently the Scherrer's crystallite size decreased consistently with Lithium doping.

Williamson-Hall (W-H) analysis of the crystallite size and strain

Though XRD peak intensities can be used to estimate the crystallite size using Debye-Scherrer equation; however, Debye –Scherrer equation is limited because it does not account for the strain in the prepared samples. There are several methods reported in the literature used to estimate crystallite size and lattice strain such as warren-Averbach, Reitveld refinement and pseudo-Voigt function. Meanwhile, the Williamson-Hall (W-H) is a simplified integral breadth method employed for estimating the crystallite size and lattice strain, thereby accounting for the strain in the samples. W-H attributed diffraction line broadening to the contributions of the crystallite size and lattice strain. The unique nature of W-H method is that it differentiates clearly between crystallite size and lattice strain peak broadening by considering the peak width as a function of 2θ (Suryanarayana and Norton, 1998).

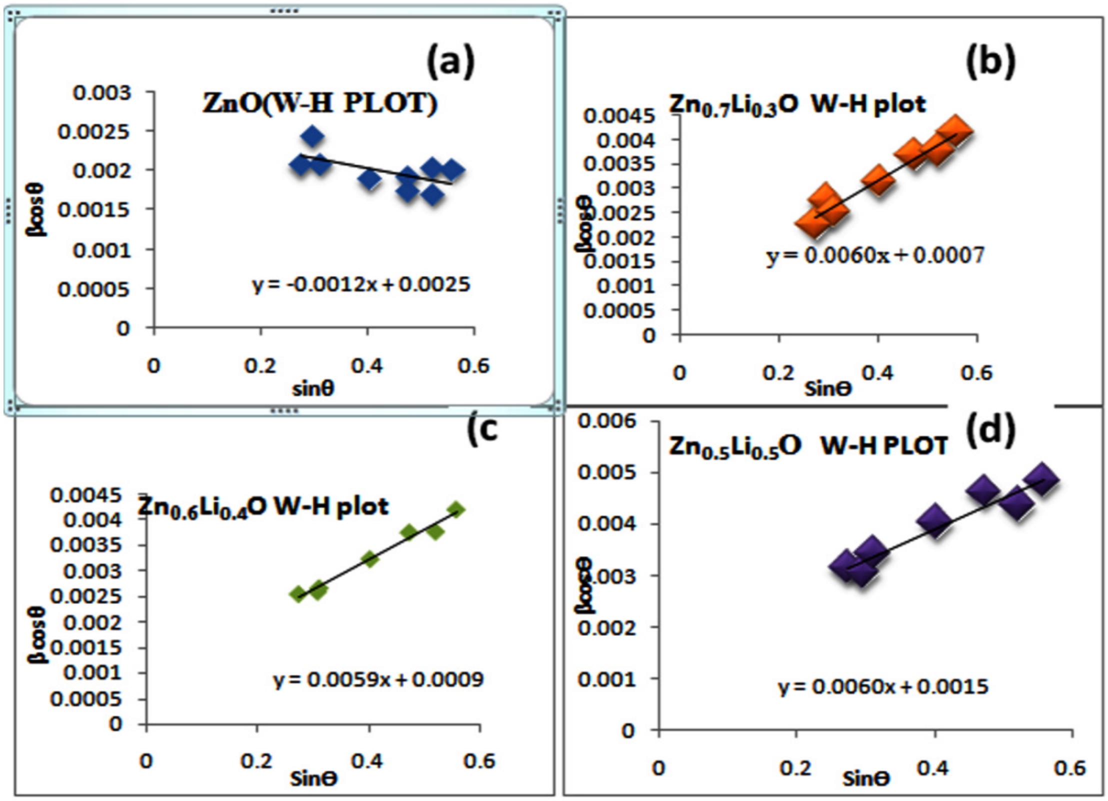

Figure 4.0: Williamson-Hall plot for all the samples (a) undopedZnO (b) $Zn_{0.7}Li_{0.3}O$ (c) $Zn_{0.6}Li_{0.4}O$ (d) $Zn_{0.5}Li_{0.5}O$

Lattice stain induced peak broadening is due to powder crystal imperfections and lattice distortion. The W-H equation given in equation (3.0) assumes that strain in the prepared samples is uniform in all crystallographic directions. The crystal is considered as isotropic in nature and it is also assumed that the properties of materials are independent of the direction of measurement (Bindu, 2014).

The values of βcosθ on y–axis were plotted as a function of Sinθ on the x–axis. The crystallite size D was estimated from the y- intercept, and the microstrain, obtained from the slope of the graphs of the linear. Figure 7.0 shows that the W-H crystallite size increased considerably in the Lithium –doped Zinc Oxide as compared to undoped Zinc oxide and then decreased systematically with increase in Lithium concentration. This is attributed to the introduction of strain in the doped Zinc oxide.

Figure 5.0 is a graph of Lattice strain and dopant concentration. The observed micro strain in the prepared samples was fairly constant and might be due to lattice mismatch as was observed in the lattice parameters.

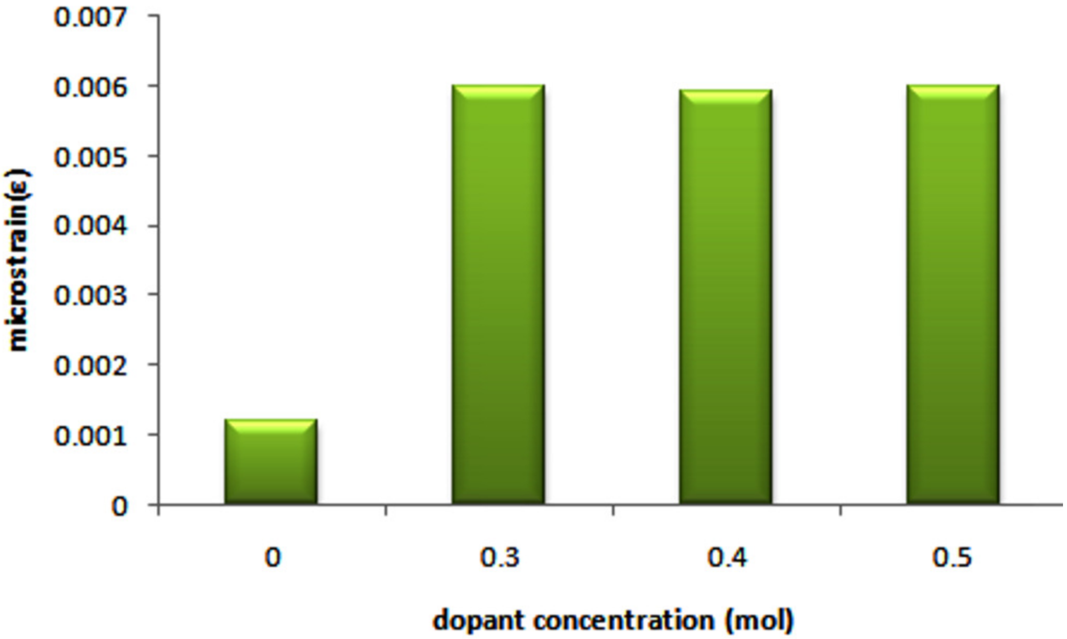

Figure 5.0: Variation of W-H micro strain with dopant concentration (a) undopedZnO (b) $Zn_{0.7}Li_{0.3}O$ (c) $Zn_{0.6}Li_{0.4}O$ (d) $Zn_{0.5}Li_{0.5}O$

Size- Strain plot

Size-strain plot has been reported as a better technique for the estimation of the crystallite size strain in the samples because less importance is given to data at high angle reflection and the data point lie very close to the linear fit. Size -strain plot is given by equation (3), and $(d\beta \cos\theta)^2$ is plotted on the vertical axis against $(d^2\beta \cos\theta)$ on the horizontal axis. The crystallite size is calculated from the gradient of the linear fit and the apparent strain computed from the intercept of the linear fit. The apparent strain is related to the root mean square strain by equation (4.0). The various size –strain plots is shown in Figure 6.0.

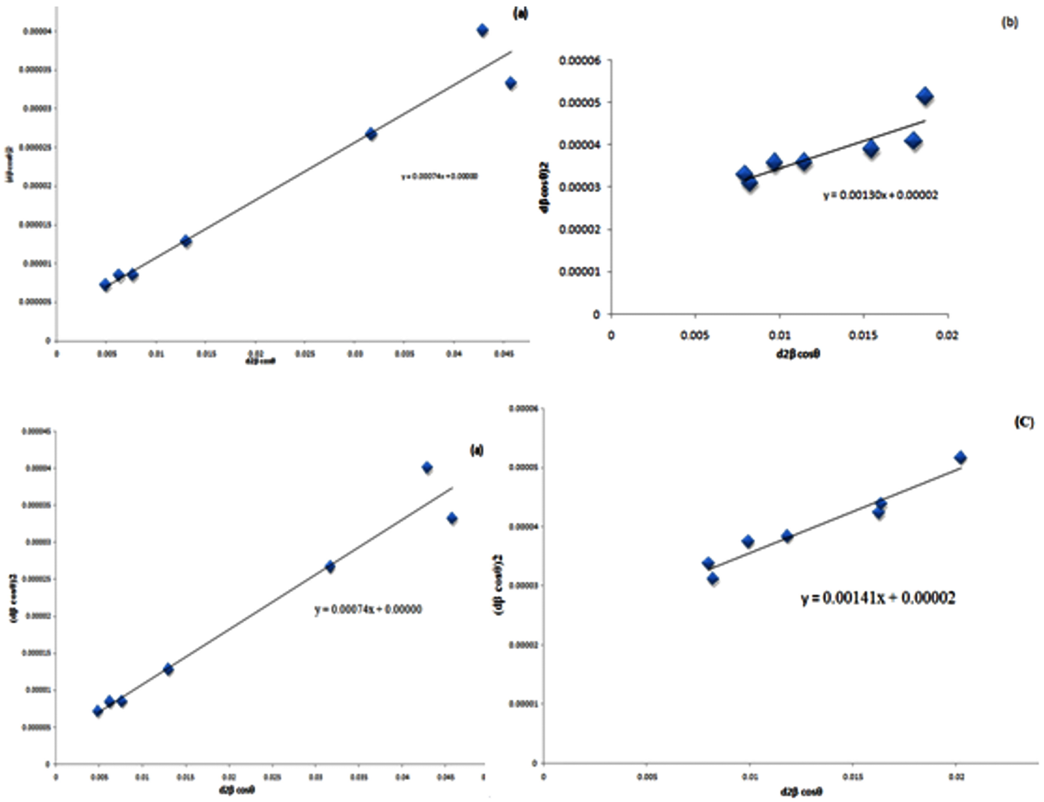

Figure 6.0: Variation of Size –Strain crystallite size (a) ZnO (b) $Zn_{0.7}Li_{0.3}O$ (c) $Zn_{0.6}Li_{0.4}O$ (d) $Zn_{0.5}Li_{0.5}O$

All the plot show a straight line fit with positive non -zero gradients. The calculated crystallite size from the gradient of the plots is shown on figure 7.0.

The crystallite size computed from this model show a systematic decease with increase in dopant concentration. The systematic decrease in crystallite size could be attributed to a higher precision in the crystallite size estimation. This follows the same trendwith W-H and Scherrer's model.

Figure 7.0: shows the composite crystallite size plot with dopant concentration

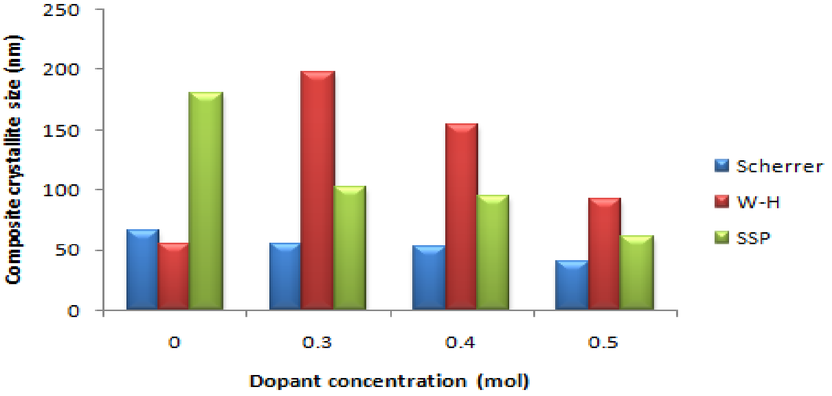

Figure 7.0: Composite plot of variation of crystallite size with dopant concentration (a) ZnO (b) $Zn_{0.7}Li_{0.3}O$(c)$Zn_{0.6}Li_{0.4}O$ (d)$Zn_{0.5}Li_{0.5}O$

Figure 7.0 shows the composite graph for the crystallite size computed using Scherrer's equation at 101 planes, W-H plot and the Size –strain plot. The graph shows that the computed crystallite size(s) followed similar trend though it is obvious that Scherrer's crystallite size is smaller than the rest which is due to neglect of the lattice contribution to peak broadening (Ashour *et al.*, 2006). It is observed that size strain crystallite size decreased systematically having variant with W-H at x= 0.0. This discrepancy raises doubt on the isotropic assumption of W-H.

Lattice Parameters

The lattice parameter 'a' for 0- 0.5 decreased from 3.256 Å to 3.243 Å while c decreased from 5.640 Å to 5.620 Å. The calculated lattice parameters are in close agreement with the standard JCPDS for zinc Oxide. The c/a ratio was constant up to the fourth decimal showing that Zinc Oxide still maintains its hexagonal wurtzite structure in spite of doping. Decrease in lattice parameters with increase in Lithium doping should be expected when Zn^{2+} ions are substituted by Li^{+} ions owing to the smaller ionic radius (0.068 Å) of Li^{+} ions to that of Zn^{2+} ions (0.074 Å). It has been reported that doping ZnO with electrically active atoms such as Lithium can cause change of lattice constant. Therefore observed decrease in lattice parameters could be attributed to Li incorporation although Khalid *et al.* (2009) attributed this to the presence of Zinc vacancies. Researcher also reported similar result (Water *et al.*, 2002).

The average grain size for the undoped Zinc Oxide is 1.23 μm while the average grain size for the Lithium- doped Zinc Oxide are 0.28 μm,0.22 μm and 0.14 μm respectively. Hence, there is a general decrease of grain size as a result of doping of Zinc Oxide with Lithium. This is shown in figure 8. Therefore, it is evident that the incorporation of Lithium inhibits the rate of grain size growth (Rakkesh and Balakuma, 2014). It has been reported that the electrical properties of material depend strongly on its grain size (Vojsavljevic, 2006), grain boundary and defects present in it. Hence, doping is a way of altering the grain size in order to increase or decrease its electrical properties. Increase in grain size reduces trapping of charged carries at the grain boundaries and also decreases the grain boundary density thereby increasing the conductivity of the material (Davood and Taha, 2009) while decrease in grain size increases the trapping and scattering of charged carriers at the grain boundaries. Hence, the observed decrease in grain size is expected to increase in resistivity of the lithium–doped Zinc. Resistivity increases in Lithium doped Zinc Oxide because Li^{+} ions act as an acceptor atom thereby reducing the charge carrier at the grain boundaries(Water *et al.*, 2002) thereby enhancing the resistivity of the material(Park *et al.*, 2002). Materials with high resistivity are a promising candidate for piezoelectric applications. David and Hsu (2008) established the relationship between piezoelectricity and resistivity. Their report shows that resistivity varies directly with piezoelectric properties in Zinc Oxide. Figure 12 (a-d) shows the composite histogram of the average grain size computed using image J software.

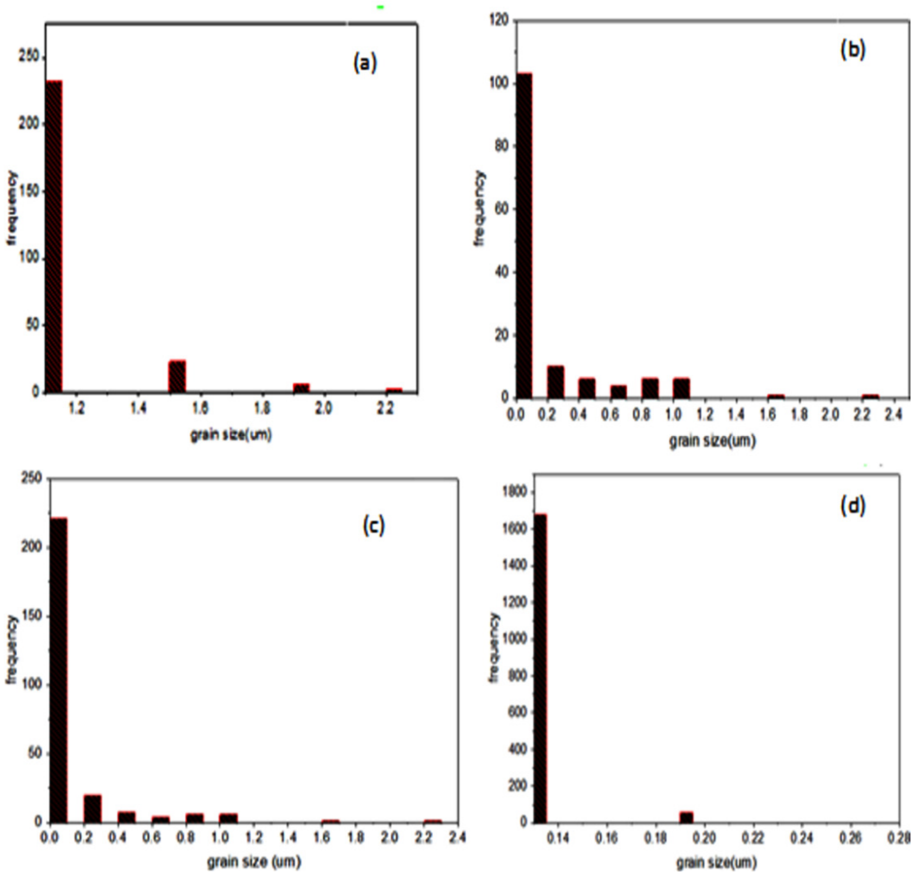

Figure 8.0: Grain distribution

The plots show that figures 8 (a and d) havemore uniform grain distributions as compared to figures 8 (b and c) which have more non-uniform grain distribution. In all the samples there is a large grain distribution at 0.00 to 0.8 μm. The computed grain size from the histogram is shown in Figure 9.

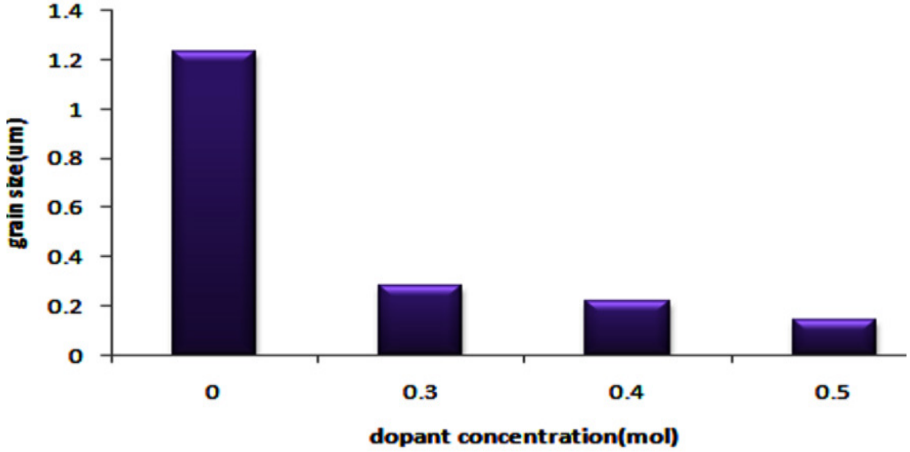

Figure 9.0: composite grain size plot: (a) x =0.00 ,grain size = 1.23 μm , (b) x= 0.3,grain size =0.28 μm (c) x= 0.4, grain size = 0.22 μm (d) x= 0.5, grain size = 0.14μm

Figure 9.0 is a plot of the average grain size against dopant concentration. It shows that pristine ZnO has the highest grain size. The Li-doped ZnO at the concentration of 0.5 mol has the least grain size. It is observed that the grain size decreased consistently with increase in Lithium doping, implying that incorporation of Lithium inhibits the growth of the grains (Rakkesh and Balakuma, 2014).

Conclusion

$Zn_{1-x}Li_xO$ ($0.00 \leq x \leq 0.05$) ceramics have been synthesised using Sol-Gel technique. Slight shifts were observed in the XRD measurement in the 2θ positions to higher and lower angles with increase in Li-doping. Peak broadening was observed in all the samples leading to small crystallite size. The average crystallite size was estimated based on corporative analysis using Scherrer's equation, Williamson-Hall and Size-strain plot. Scherrer's crystallite size has the least values due to the neglect of the strain contribution to crystallite sizes. The calculated crystallite sizes from all the models followed similar trend and follow similar trend.

Decrease in crystallite size was observed in all the samples. The lattice parameters (*a* and *c*) showed slight anisotropic contraction. General decrease in the unit cell volumes and bond lengths were observed in all the grains. The shape of the samples changed from spherical to rod-like as dopant concentration increased. Agglomeration, non-uniform distribution of grains and porous regions were observed in x = 0.00, 0.3 and 0.4 sample at various degrees. The grain size shows a decreasing trend with increase in lithium concentration. The optimum doping in this study was found to be 0.5 mol. which corresponds to the lowest grain size thus having the potential for piezoelectric application.

References

Ahmed, W. M., Abdel-Hameed, A. R., Moghazy, F. M. E. (2008). Some reproductive and Health aspect of female buffaloes in relation to lead concentration. *Int.J.Dairy Sci.*, 3(2), 63-70.

Ashour, A., Kaid, M. A., El-Sayed, N., & Ibrahim, A. A. (2006). Physical properties of ZnO thin film deposited by spray pyrolysis technigue. *Applied Surface Science,* 252,7844-7848.

Ardyanian, M., & Sedigh, N. (2013). Heavy Lithium doped thin films prepared by spray pyrolysis. School of Physics and Center for solid state physics research, Damghan University, Damghan, Iran.

Bilgin, V. (2009). Preparation and characterisation of ultrasonically sprayed zinc oxide thin films doped with lithium. *Journal of Electronic Material*, 88(9), 1969 – 1978.

Bindu, P., & Thomas, S. (2014). Estimation of lattic strain in ZnO profile analysis. *Journal of Theoretical and Applied Physics,* 8,123-134. doi: 10.1007/s40094-014-0141-9.

Corsol, D., Andrea, P., Michel, R.., & RaffaeleBaldereschi, A. (1994). Ab initio study of piezoelectricity and spontaneous polarisation in ZnO.*Physical Review Publisher*, 50(15), 10715-10721.

Dai, S. H., & Park, H. S. (2013). Surface effect of piezoelectricity of ZnO Nanowire*. Journal of Mechanics and Physics of Solids,* 61,385-397.

David, A. S., & Hsu, J. W. P. (2008). Effect of Lithium doping on microstructural and optical properties of ZnONanocrystalline films prepared by sol-gel method. Nanoletters, 8. Available at http://doi:org/10.1021/108074

Davood, R., & Taha, R. (2009). The effect of heat treatment on the physical properties of solgel derived ZnO thin films. Applied Surface Science Journal, 255, 58125817. Doi: 10,1016/j.apsusc.2009.01.010

Du, Y. L., Deng, Y., & Zhang, M. S. (2005). Investigation of Li-Induced Structural disorder and phase transition in ZnO by Raman spectroscopy. *Solid State Communications Journal,* 137, 78-81, doi:10.1016/j.ssc.2005.10.002

Khan, M. K. R., Rahman, M. M., & Tanaka, I. (2003). Preparation, Structuraland Electrical Properties of $Zn_{1-x}Li_xO$ solid solution. *The nucleus journa*l, 39, 3-4,149-154

Lina,Y.J.,M.S.Wang M.S.,.Liub,C.J.,Huanga,H.J.(2010) "Defects, stress and abnormal shift of the (002) diffraction peak for Li-doped ZnO films", *Applied Surface. Science,* 256 (2010) 7623–7627

Lou, X. (1991). Development of ZnO series ceramic semiconductor gas sensors. *Journal of Transducers Technology.*

Nayak, P. K., Jang, J., Lee, C., & Hong, Y. (2009). *Applied Physics Letter,* 95, 193503.

Park, C. H., Zhang, S. B., & Wei, S. H. (2002). Origin of p-type doping difficulty in ZnO: The impurity perspective. *Physical Review,* 66. Article ID 073202.

Prasad, S. E., Waechter, D. F., Richard, G. B., King, H. W., & Yavuz, Y. (2005). 11 elomas thematics. *Conference on smart Structure and Materials.*

Rakkesk, R. A., & Balakumar, S. (2014). Processing and application of ceramics. 7-*Review Letters*, 82(12), 2552-2555.

Segets, D.; Gradl, J.; Taylor, R.K.; Vassilev, V.; Peukert,W (2009)3,1703-1710 Analysis of optical absorbance spectra for the determination of ZnO nanoparticle size distribution, solubility, and surface energy. *American Ceramics Society* (2009) 3, 1703-1710.

Suryanarayana, C., & Norton, M. G. (1998). *X- ray diffraction: A practical approach.* New York: Plenum press publishing.

Vojisavijevic, K., Zunic, M., Brankovic, G., & Sreckovic, T. (2006). Electrical properties of mechanically activated zinc oxide. *Science of Sintering Journal*, 38,131-138. doi: 10.2298/SOS0602131V.